scientific reports

Check for updates

OPEN

Elucidating the role of KCTD10 in coronary atherosclerosis: Harnessing bioinformatics and machine learning to advance understanding

Xiaomei Hu[1,2], Fanqi Liang[3], Man Zheng[4], Juying Xie[1,2,5]✉ & Shanxi Wang[1,2,5]✉

Atherosclerosis (AS) is increasingly recognized as a chronic inflammatory disease that significantly compromises vascular health and serves as a major contributor to cardiovascular diseases. KCTD10, a protein implicated in a variety of biological processes, has garnered significant attention for its role in cardiovascular diseases and metabolic regulation. As a member of the KCTD protein family, KCTD10 is characterized by the presence of a T1 domain that interacts with voltage-gated potassium channels, a critical interaction for modulating channel activity and intracellular signal transduction. In our study, KCTD10 was identified as a focal point through an integrative analysis of differentially expressed genes (DEGs) across multiple datasets (GSE43292 and GSE9820) from the GEO database, aligned with immune-related gene sets from the ImmPort database. Advanced analytical tools, including Lasso regression and Support Vector Machine-Recursive Feature Elimination (SVM-RFE), were employed to refine our gene selection. We further applied Gene Set Enrichment Analysis (GSEA) and Gene Set Variation Analysis (GSVA) to these gene sets, revealing significant enrichment in immune-related pathways. The relationship between KCTD10 expression and immune processes was examined using CIBERSORT and ESTIMATE algorithms to assess tumor microenvironment characteristics, suggesting increased immune cell infiltration associated with higher KCTD10 expression. Validation of these findings was conducted using data from the GSE9820 dataset. Among 10 DEGs linked with KCTD10, 13 were identified as hub genes through LASSO and SVM-RFE analyses. Functional assays highlighted KCTD10's role in enhancing viral defense mechanisms, cytokine production, and immune cascades. Notably, KCTD10 expression correlated positively with several immune cells, including naive CD4 + T cells, eosinophils, resting NK cells, neutrophils, M0 macrophages, and particularly M1 macrophages, indicating a significant association. This research elucidates the complex relationship between KCTD10 and AS, underscoring its potential as a novel biomarker for diagnosing and monitoring the disease. Our findings provide a solid foundation for further investigations, suggesting that targeting KCTD10-related pathways could markedly advance our understanding and management of AS, offering new avenues for therapeutic intervention.

Keywords Coronary Atherosclerosis (AS), *KCTD10*, Lasso regression, SVM-RFE, Autoimmune inflammatory disorder

Coronary artery disease (CAD), a primary cause of global mortality, accounted for nearly 18 million deaths in 2017, with projections suggesting an escalation to 23.4 million by 2030[1]. The development of CAD is closely associated with the formation of atherosclerotic plaques, leading to coronary obstruction, myocardial ischemia, and tissue necrosis, thereby increasing the risk of acute cardiovascular syndromes (ACS)[2]. There has been a

[1]College of Medical Imaging Laboratory and Rehabilitation, Xiangnan University, Chenzhou 423000, Hunan, China. [2]Rehabilitation Department, Affiliated Hospital of Xiangnan University, No.25, People's West Road, Chenzhou 423000, Hunan, China. [3]The First Affiliated Hospital of Hunan University of Traditional Chinese Medicine, Changsha 410007, Hunan, China. [4]Dongying People'S Hospital (Dongying Hospital of Shandong Provincial Hospital Group), Dongying, Shandong 257091, People's Republic of China. [5]Juying Xie and Shanxi Wang contributed equally. ✉email: 597189746@qq.com; evy_i@qq.com

notable increase in atherosclerosis (AS) prevalence in recent years, a trend often linked to dietary habits high in fats and sugars but low in fiber, presenting significant public health challenges[3]. AS, a chronic inflammatory arterial disease, begins with inflammatory processes in the arterial intima, characterized by the infiltration and retention of low-density lipoprotein (LDL) in the arterial walls, leading to the formation of atherosclerotic plaques comprised of inflammatory cells and LDL deposits. Despite extensive research, the genomic regulatory mechanisms of AS are still not fully understood[4]. The field of metabolism, encompassing essential biochemical reactions, plays a critical role in the onset and progression of various diseases, including metabolic, oncological, and cardiovascular disorders[5]. The disruption of metabolic pathways is a common pathological aspect of these diseases. Recent developments in metabolic research have shed light on the intricate links between metabolic processes and disease progression, revealing new therapeutic targets and biomarkers[6]. Moreover, the vital role of metabolism in modulating immune responses and inflammation is gaining recognition[7]. Metabolic pathways critically influence immune cell function, affecting their differentiation, activation, and efficacy. Alterations in immune cell metabolism are increasingly identified as contributors to autoimmune diseases, chronic inflammatory conditions, and compromised defenses against pathogens[8].

KCTD10 (potassium channel tetramerization domain containing 10) is a protein implicated in a variety of biological processes, with its role in cardiovascular diseases and metabolic regulation garnering significant attention. As a member of the KCTD protein family, KCTD10 is characterized by the presence of a T1 domain that interacts with voltage-gated potassium channels, a critical interaction for modulating channel activity and intracellular signal transduction[9]. Recent scientific endeavors have focused on elucidating the molecular mechanisms by which KCTD10 influences cardiovascular system functionality[10]. Studies have demonstrated that KCTD10 modulates vascular morphology and function through its impact on lipid metabolism and cholesterol transport, playing a pivotal role in the development of AS[11]. Additionally, the association of KCTD10 with cardiovascular diseases has sparked clinical interest, particularly in exploring its potential as a therapeutic target. At the molecular level, KCTD10 influences a variety of signaling pathways, including those related to lipid and cholesterol metabolism, underscoring its importance in cellular homeostasis, particularly in cardiovascular health and disease[12]. Despite significant advancements in KCTD10 research, numerous critical questions remain unanswered. For instance, the interaction network of KCTD10 with other proteins, its specific mechanisms of action in various physiological and pathological states, and how these mechanisms can be precisely modulated to treat related diseases are current focal points of research[13]. Future studies will continue to delve into the role of KCTD10 in cell biology and how it influences fundamental cellular processes affecting the health of the entire organism. Growing evidence suggests that KCTD10 plays a pivotal role in key pathways implicated in AS, such as vascular smooth muscle cell proliferation, endothelial barrier integrity, and inflammatory signaling cascades. Investigating the mechanistic link between KCTD10 and AS is essential to unravel novel pathophysiological insights and identify therapeutic targets for this life-threatening condition.

Recent cancer research has revealed a distinct metabolic phenotype in tumor cells, reshaping the immune microenvironment. This environment, defined by cellular heterogeneity and resource limitations due to impaired vascularization, has spurred renewed interest in the role of non-neoplastic immune components[14]. Evidence suggests that oncogenic transformation endows tumor cells with a unique metabolic profile, profoundly altering the immune landscape. The immune microenvironment is a dynamic network of diverse cell types within a dysregulated extracellular matrix, characterized by oxygen and nutrient deprivation stemming from aberrant vasculature[15]. Increasing immune infiltration into non-malignant regions further complicates this system. The interplay between immune responses and metabolic rewiring in tissues is marked by nutrient scarcity, enhanced oxygen consumption, and the production of reactive nitrogen and oxygen species, all of which influence immune effector cell function[16]. This crosstalk indicates that targeting metabolic pathways could potentiate the effectiveness of immunotherapies. Understanding the link between metabolism and immune regulation is pivotal for advancing cancer immunotherapy[17]. The integration of high-throughput data analytics and bioinformatics is transforming the study of gene function networks across diseases, yielding critical insights into complex molecular mechanisms[18]. The wealth of transcriptomic data, coupled with clinical insights from initiatives such as the AS Initiative, provides an unparalleled opportunity to investigate disrupted transcriptional landscapes and molecular cascades in AS[19,20]. Despite these advances, bioinformatics remains underutilized in dissecting AS within its intricate disease context. This study aims to fill this gap by analyzing AS-associated datasets from the GEO repository, focusing on the molecular framework of AS to enhance our understanding of its mechanisms. This approach seeks to uncover the complex molecular networks and pathways in AS, potentially informing novel therapeutic interventions (Fig. 1).

Materials and methods

We used the approaches proposed by Zi-Xuan Wu, et al. 2023[21]. This study leveraged publicly available GEO datasets to elucidate the role of GlnMgs in Alzheimer's disease (AD). Differential expression analysis and risk model construction were conducted using GSE132903 as the primary dataset, with GSE63060 employed for validation and classification refinement. Prognosis-associated GlnMgs were identified, and their biological functions were characterized through GO, KEGG pathway analysis, and GSEA. Furthermore, immune cell infiltration, functional pathways, and RNA expression alterations were systematically analyzed, providing a comprehensive perspective on the involvement of GlnMgs in AD pathogenesis.

Source of transcriptional profiling data

The GEO, established and maintained by the NCBI, is a comprehensive public repository for high-throughput gene expression data submitted by research institutions globally. Since its inception in 2000, GEO has become an essential resource, encompassing data derived from a range of technologies, including microarray arrays and next-generation sequencing, with all datasets freely accessible to the scientific community. In cases where multiple

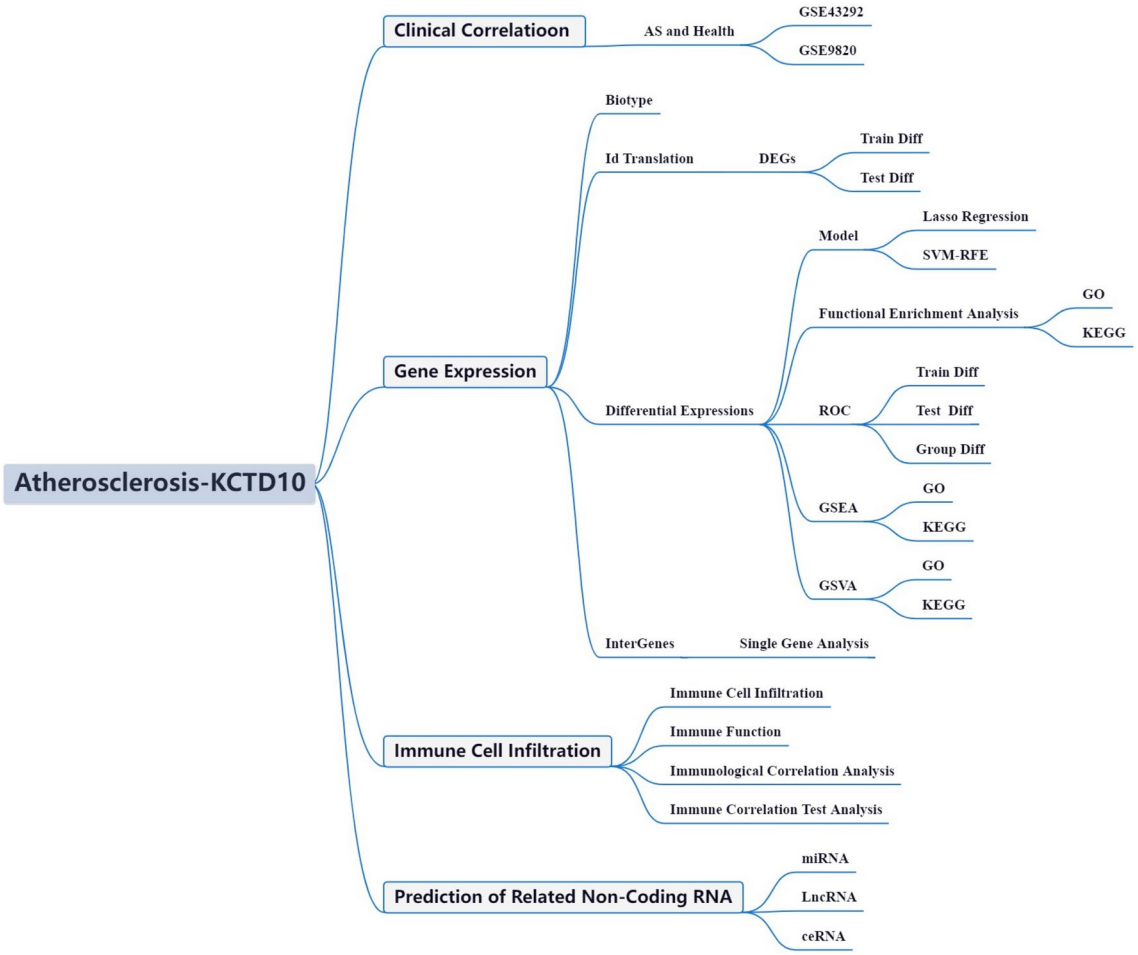

Fig. 1. Framework. Through integrative analysis of DEGs derived from multiple datasets, including GSE43292 and GSE9820 from the GEO database, and immune-related gene sets from the ImmPort database, we identified KCTD10 as a pivotal gene in the context of immune regulation. To enhance the precision of gene selection, we employed advanced methodologies such as Lasso regression and SVM-RFE. GSEA and GSVA further revealed substantial enrichment in immune-related pathways. Additionally, using the CIBERSORT and ESTIMATE algorithms, we investigated the association between KCTD10 expression and immune processes, uncovering a positive correlation between elevated KCTD10 expression and enhanced immune cell infiltration.

GSE43292		GSE9820	
Variables	**Number of samples**	**Variables**	**Number of samples**
Gender Male/Female Diagnosis	unknown	Gender Male/Female Diagnosis	64/89
AS/No-AS Tissue	32/32	AS/No-AS Tissue	87/66
Macroscopically intact tissue/ Atheroma plaque	32/32	Macroscopically intact tissue/ Atheroma plaque	unknown

Table 1. The clinical characteristics of patients.

probes corresponded to a single gene, the arithmetic mean of these probe values was calculated to represent the gene's overall expression level. Data normalization was performed using the Sva and Limma packages of R4.1.0, specifically designed for multi-chip batch correction. Following this, batch effect normalization was further refined using the SVA package, and the effectiveness of this correction was assessed by Principal Component Analysis (PCA). Differential expression analysis between AS and control groups was conducted using the Limma package, with differentially expressed genes (DEGs) defined by an absolute log fold change (|log FC|) greater than 1 and an adjusted p-value of less than 0.05. This approach enabled the identification of genes associated with immune infiltration in AS. The datasets GSE43292 and GSE9820 were employed, with the former serving as the training cohort and the latter as the test cohort (Table 1). Gene expression data were derived from platforms GPL6244 and GPL6255. In addition, we identified genes involved in fatty acid metabolism (Table S1).

Predictive modeling and computational learning

In our endeavor to construct a predictive model with unparalleled precision and reliability, we adopted the glmnet package to implement Lasso regression, enhanced through rigorous cross-validation[22]. This strategy effectively mitigated overfitting and heightened the model's predictive accuracy across complex biological datasets. To extend our validation, we employed the advanced SVM-RFE algorithm via the e1071 package, meticulously engineering a robust machine learning model. Cross-validation was pivotal in scrutinizing the model's error rates and precision, bolstering its robustness and dependability. Further enhancing our analysis, the Random Forest algorithm analysis was also used It generated numerous decision trees and integrated their outcomes, thereby reducing overfitting and augmenting the model's generalization. A salient feature of this method—random selection of features and bootstrap sampling—enriched the diversity among decision trees, thereby elevating the overall model accuracy[23,24]. Then, the DEGs obtained before were calculated by different algorithms, and then intersected by VNN package to obtain the key genes, so as to construct the model. Utilizing the randomForest and ggplot2 packages, our focus on the analysis of DEGs, pinpointing pivotal genes for AS. In the final phase, we assessed the importance of these genes through an integrated approach that amalgamated insights from Lasso regression and SVM models. The genes identified through these comprehensive methodologies are now primed for further exploratory analysis. The AUC (area under the curve) value of 1.0 denotes an ideal diagnostic test, whereas an AUC close to 0.5 indicates a lack of discriminative power, equating to random chance. This metric is particularly valuable for assessing the diagnostic accuracy of medical tests and the predictive reliability of models at different thresholds. In our analysis, we utilized the R pROC package to integrate and evaluate the dataset combining AS outcomes with pivotal genes to assess their predictive accuracy. Additionally, the dataset GSE9820 was employed to validate these findings. Through the ROC curve, we established a robust methodological framework for evaluating the diagnostic performance of these biomarkers, thus enhancing our understanding of their potential utility in clinical settings.

Functional enrichment analysis

To elucidate the biological functions and signaling pathways involved in the differential expression landscape, we conducted GO and KEGG analyses. Using the R statistical environment, we explored how variations in KCTD10 expression influence BP, MF, and CC. Global gene-set enrichment analyses, including GSEA and GSVA, were employed to identify functionally coherent gene sets and signaling pathways differentially active in the studied samples. Enrichment scores and visual representations were generated to reveal dynamic activities and pathways across different risk stratifications. The R environment was used to investigate the impact of differential KCTD10 expression on BP, MF, CC, and related pathways.

Active components-targets predictive

KCTD10 were docked to verify the accuracy of principal components and prediction targets. The protein configurations of the core targets were obtained from the Uniprot database by using the minimum resolution (Resolution) and the source (Method) as X-ray as the screening condition, and the crystal structure of these protein configurations were obtained from the RCSB PDB database). 2D structures of active components of core targets were obtained from PubChen database, and these 2D structures were minimized by chem3d software. The binding strength and activity of active components and targets were evaluated by SYBYL2.0 software, and the active components of binding TotalScore greater than 3 were selected for sub-docking.

Biomarker-immune infiltrate and miRNA-lncRNA network

Spearman's rank correlation was employed to assess the relationship between diagnostic biomarkers and immune cell infiltration within the tissue microenvironment. We used R's limma, GSVA, GSEABase, ggpubr, reshape2 packages to match and calculate KCTD10 and immune-related data. These included removal of control samples, ssgsea analysis and correction of scores for immune-related functions. Finally, the samples will be grouped according to the KCTD10. Target gene information for the common miRNAs and lncRNAs was obtained from miRTarbase and PrognoScan databases. These databases include miRanda[25], miRDB[26], and TargetScan[27]. When the corresponding database matched the relevant miRNA, the score was marked as 1. It can be seen that when all three databases can be matched, it is 3 points. The miRNA was matched by spongeScan database[28] to obtain the corresponding lncRNA data. An integrated regulatory network, highlighting the interplay between mRNAs, miRNAs, and lncRNAs along with their shared targets in AS, was constructed and visualized using Cytoscape software. In addition, to unravel the fundamental mechanisms underlying KCTD10, we constructed a comprehensive Gene regulatory networks from GeneMANIA.

Establishing causality via mendelian randomization

In our endeavor to ascertain the non-confounded relationship between genetic predispositions and AS incidence, a Mendelian randomization study was conducted, leveraging the TwoSampleMR package within R. This analysis aimed to explore the potential causal linkage between KCTD10 gene expression—designated as the exposure variable—and AS, identified as the outcome of interest. (1) IV Selection: We pinpointed KCTD10 expressions closely linked to the exposure, employing a stringent significance cutoff of $P < 5 \times 10^{-8}$ to ensure the relevance of the chosen genetic instruments. (2) Ensuring Independence of IVs: To ascertain the independence of SNPs serving as risk factors, we utilized the PLINK clustering methodology to examine LD. SNPs were screened for LD, with those exhibiting an LD coefficient (r^2) greater than 0.001 or a physical proximity of under 10,000 kilobases being excluded. This step was crucial to uphold the independence of SNPs and mitigate the risk of pleiotropy that could confound causal inferences. (3) Statistical Robustness of IVs: The integrity of each instrumental variable was scrutinized through the calculation of the F-statistic ($F = \beta^2/SE^2$), where β represents the effect

size of the allele, and SE is the standard error. Instrumental variables demonstrating an F-value less than 10 were disregarded to reduce the likelihood of bias introduced by latent confounders.

Statistical considerations

Statistical assessment of gene expression disparities between the distinct cohorts was executed via the ggpubr package in R (version 4.3.1). For data adhering to a normal distribution, two-sample independent t-tests were utilized; alternatively, the Wilcoxon rank-sum test was applied for non-normally distributed data. A p-value threshold of less than 0.05 was deemed statistically significant for all tests.

Results

DEG identification and principal component analysis

We integrated GSE43292 and GSE9820 and conducted batch match evidence integration. PCA corroborated the successful demarcation of patients into risk-specific cohorts (Fig. 2a-b). Among the 2798 DEGs, some DEGs were found to be significantly different. In addition, Some genes cluster in the treat group and some in the control group. Treat: DPP3, ADCY4, VAV1, CNDP2, RIPK3, ITGAL, PLCB2, PSME1, TAP1, PARP12, STAT1, etc. Control: CALD1, MYLK, MYL9, WASF3, PDE5A, SPARC, PGRMC1, PROS1, MAOB, CDC14B, etc. (Fig. 2c). Some of these DEGs were significantly up-regulated (C1QB and C1QA). However, some genes were significantly down-regulated (SPARC, PROS1, CTNNAL1, GNG11 , MEIS1, FSTL1, SH3BGRL2 , C1QB, JAM3). (Fig. 2d). (Table.S1).

Construction of the model

To construct a robust gene signature for AS, we employed LASSO and Cox regression analyses to optimize gene selection, as demonstrated in Figs. 3a and 3b. Subsequently, the SVM-RFE technique was utilized to develop a machine learning model, confirming the model's high accuracy and reliability with an accuracy rate of 0.696 and an error rate of 0.304 (Figs. 3c and 3d, Table 2). Further investigation using Random Forest analysis identified several key genes (Figs. 3e). These DEGs were then analyzed through a comprehensive approach using Lasso regression, SVM-RFE, and Random Forest algorithms. This integrated analytical strategy successfully pinpointed 23 critical hub genes,, confirmed by consensus among the outputs from the three methodologies (Fig. 3f; Table S2). Based on these results, *KCTD10* was selected for in-depth analysis, underlining its potential significance in the pathophysiology of AS.

DEG identification and visualization

We visualized these 23 hub genes in the AS group and the normal sample group respectively (Fig. 4). In the confirmation of 23 hub genes, we analyzed the ROC of these genes, showing that the accuracy of these genes is high. SF3B3 (AUC:0.665), KLRD1 (AUC:0.639), ASPA (AUC:0.650), LGALS3BP (AUC:0.638), RABEP1 (AUC:0.614), STYK1 (AUC:0.621), SDK2 (AUC:0.622), NDFIP1 (AUC:0.613), IMPA1 (AUC:0.609), PKD1L3 (AUC:0.622), OR2T8 (AUC:0.608), DAOA (AUC:0.596), C10orf111 (AUC:0.612), WDR77 (AUC:0.612), UBE2L3 (AUC:0.613), KCNA10 (AUC:0.600), KLHL10 (AUC:0.504), KCTD10 (AUC:0.586), TAS2R38 (AUC:0.589), SPANXB1 (AUC:0.591), OR56B4 (AUC:0.569), LRRC19 (AUC:0.583), MT1H (AUC:0.545). (Fig. 5).

Validation of hub genes

GSE9820 was used for validation to boost our model's confidence and prediction accuracy of these hub genes. What's interesting is that these DEGs are showed significant differences in GSE9820 analysis (Fig. 6a). In the

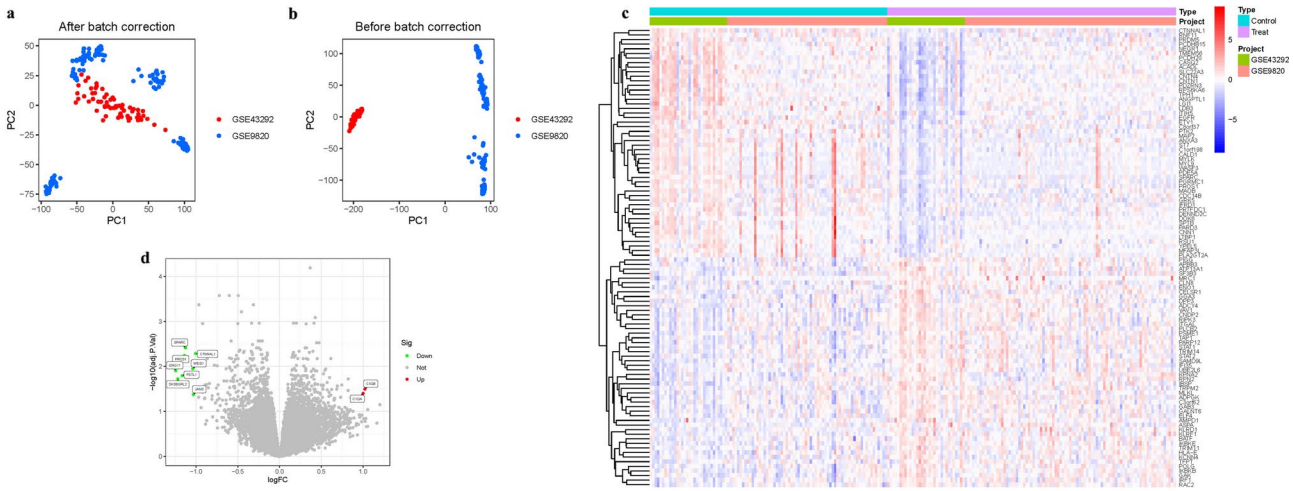

Fig. 2. Principal Component Analysis. (**a-b**) Analysis of PCA. According to the distribution of the red and blue points in the graph. It can be seen that the data of the two groups are well stratified. They don't overlap. This represents no large result bias after normalization of our data. (**c**) Heatmap. (**d**) Volcano map.

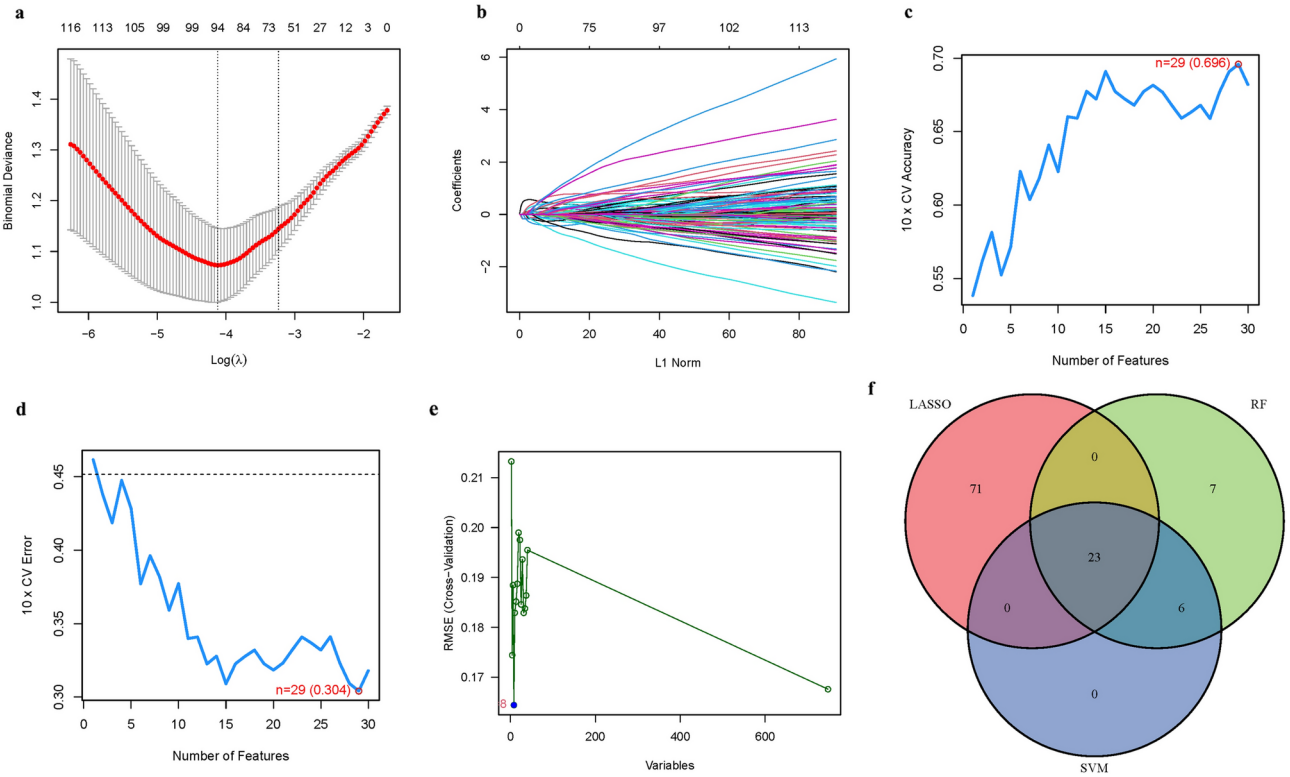

Fig. 3. The development of the signature. (**a**): Regression of the AS-related genes using LASSO. (**b**): Cross-validation is used in the LASSO regression to fine-tune parameter selection. (**c-d**): Accuracy and error of this model. (**e**): Random forest analysis. (**f**): Venn.

Label	LASSO	SVM-RFE	RF
Sensitivity	0.417	0.500	0.392
Specificity	0.800	1.000	0.918
Pos Pred value	0.556	1.000	0.429
Neg Pred value	0.696	0.769	0.900
Precision	0.556	1.000	0.429
Recall	0.417	0.500	0.375
F1	0.476	0.667	0.400
Prevalence	0.375	0.375	0.140
Detection rate	0.156	0.188	0.053
Detection prevalence	0.281	0.188	0.123
Balanced accuracy	0.608	0.750	0.647

Table 2. The characteristics of model.

GSE9820 analysis of hub genes, we analyzed the ROC of these genes, showing that the accuracy of these genes is high. SF3B3 (AUC:0.831), KLRD1 (AUC:0.741), ASPA (AUC:0.774), LGALS3BP (AUC:0.750), STYK1 (AUC:0.752), SDK2 (AUC:0.755), NDFIP1 (AUC:0.794), PKD1L3 (AUC:0.714), WDR77 (AUC:0.748), KCTD10 (AUC:0.820), TAS2R38 (AUC:0.723. These results also confirmed the high reliability and accuracy of our model (Fig. 6b).

Differential expression and enrichment analysis centered on KCTD10

KCTD10 was selected as a key investigative gene to determine its unique contributions to AS. Utilizing differential expression analysis focused on this gene, we identified 10 DEGs linked to *KCTD10*, as illustrated in Fig. 7. These DEGs varied significantly in expression, with certain genes predominating in distinct expression clusters. The 'high' expression cluster included notable genes such as FUCA1, C1QC, SLC29A3, FAM78A. Conversely, the 'low' expression cluster comprised genes like PDLIM1, COBLL1, LRIG1, GEM, EXT1, TJP2 (Figs. 7a-b). Additionally, we developed a correlation matrix to further explore the relationships between *KCTD10* and these DEGs, providing a detailed visualization of these associations (Fig. 7c) and catalogued in Supplementary Table

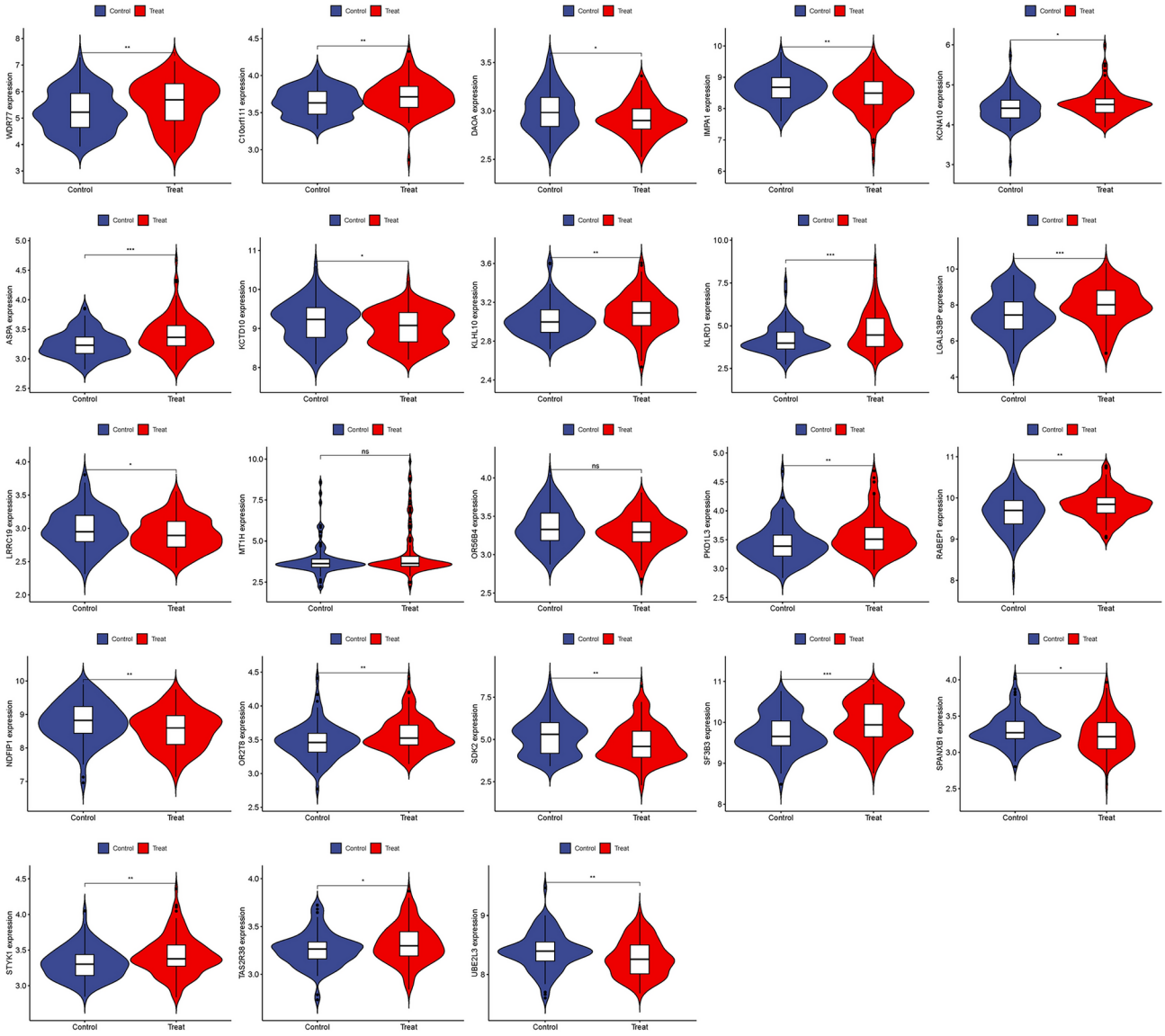

Fig. 4. Expression of 23 hub genes in AS group and normal sample group respectively.

S3. This analysis not only highlights the differential roles of *KCTD10* in AS but also maps its potential regulatory network, offering insights into its biological and pathological roles. GO enrichment identified 65 principal targets categorized under MF and BP. The MF category was predominantly associated with cytokine binding, non – membrane spanning protein tyrosine kinase activity, immune receptor activity. BPs included response to response to regulation of immune effector process, cell activation involved in immune response, mononuclear cell differentiation. CC was predominantly associated with vesicle lumen, cytoplasmic vesicle lumen, secretory granule membrane. In the context of AS, these findings suggest a direct mechanistic link between immune regulation and disease pathogenesis. AS is characterized by chronic inflammation and immune cell infiltration, processes that are critically influenced by cytokine signaling, immune receptor activation, and mononuclear cell differentiation. Disruption in vesicle trafficking or secretory granule function may impair cytokine release or receptor localization, exacerbating inflammatory responses and promoting plaque progression. We hypothesize that targeting these molecular and cellular pathways could offer novel therapeutic opportunities to mitigate immune-driven inflammation in AS, paving the way for more precise interventions in this complex disease.

KEGG pathway analysis reveals that overexpressed genes are significantly enriched in pathways such as cytokine-cytokine receptor interaction (hsa04060), the PI3K-Akt signaling pathway (hsa04151), and lipid and atherosclerosis (hsa05417). These pathways are pivotal in regulating immune and inflammatory responses, lipid metabolism, and cellular survival, all of which are fundamental processes implicated in the progression of AS. The integration of these findings, as depicted in Fig. 7d-e and Table S3a-b, underscores the multifaceted role of these pathways in mediating the crosstalk between inflammation and vascular pathology. KCTD10 emerges as a critical regulator within this network, influencing immune responses and inflammation through its impact on these pathways. Specifically, cytokine-cytokine receptor interactions and PI3K-Akt signaling are known to modulate

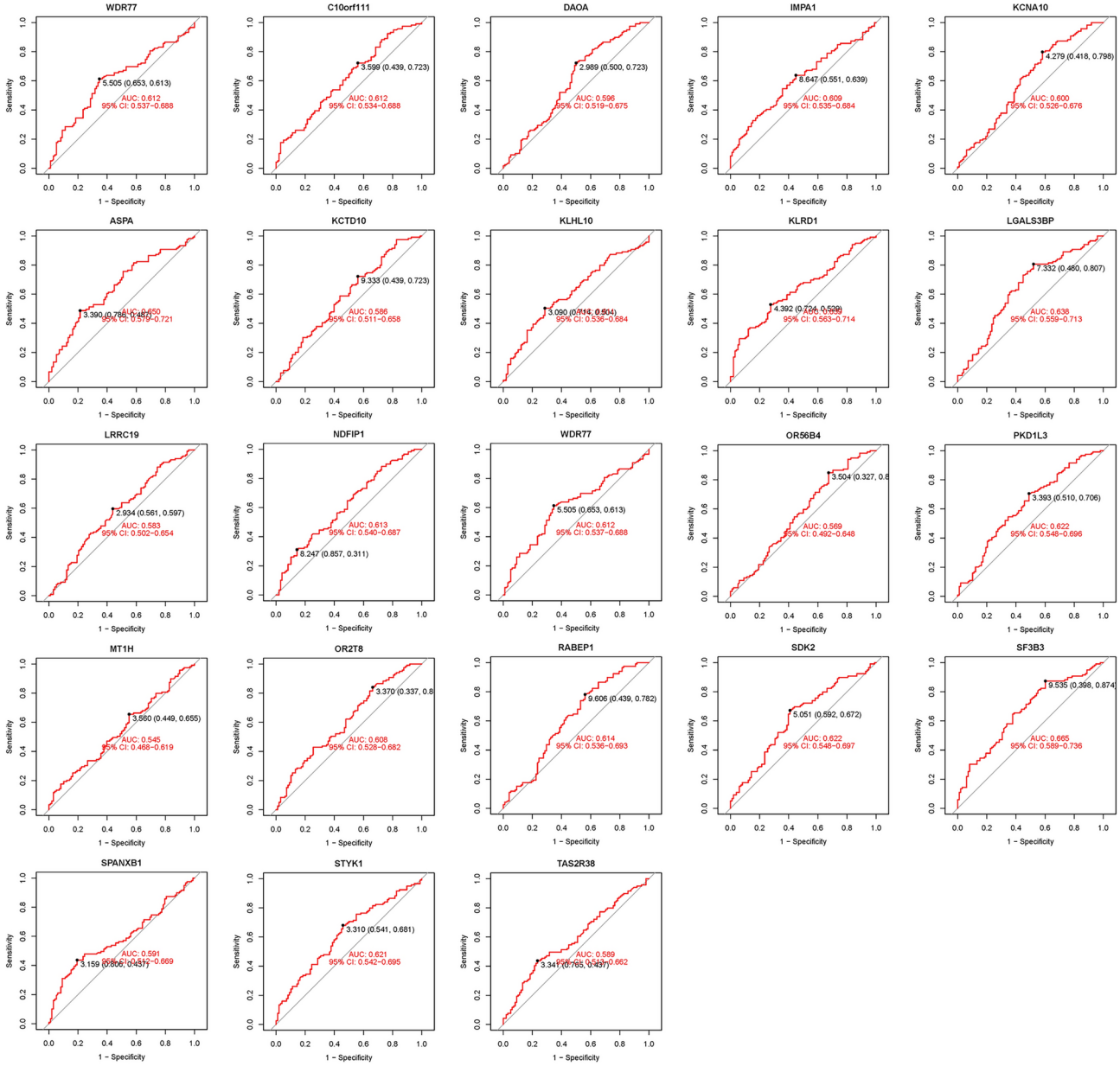

Fig. 5. ROC of 23 hub genes.

vascular inflammation, endothelial dysfunction, and macrophage activation—key drivers of AS development. Moreover, the association of KCTD10 with lipid and atherosclerosis pathways suggests its potential involvement in lipid homeostasis and foam cell formation, further contributing to plaque formation and progression. We hypothesize that KCTD10 mediates AS pathology through its regulation of these interconnected pathways, with dysregulation potentially amplifying inflammatory and metabolic derangements characteristic of the disease. Future studies focusing on the mechanistic role of KCTD10 in these pathways could uncover novel therapeutic targets to mitigate immune-driven inflammation and lipid dysregulation in AS.

GSEA and GSVA analysis of KCTD10

To elucidate the biological functions impacted by differential expression of *KCTD10*, we applied GSEA using an array of computational tools including limma for differential expression analysis, org.Hs.eg.db for gene annotation, clusterProfiler and enrichplot for visualization of enrichment results. GSEA facilitated the identification of significant functional alterations among the DEGs linked to *KCTD10*. In the analysis of GO categories for the high expression group, enrichment was CC actin cytoskeleton, CC contractile fiber , CC filamentous actin. Conversely, in the low expression group, functional enrichments were noted in BP leukocyte mediated immunity, BP myeloid leukocyte activation , CC tertiary granule (Fig. 8a). In the context of AS, these findings suggest a dual mechanistic influence on vascular and immune homeostasis. High expression, characterized by cytoskeletal enrichment, may reflect altered endothelial or smooth muscle cell mechanics,

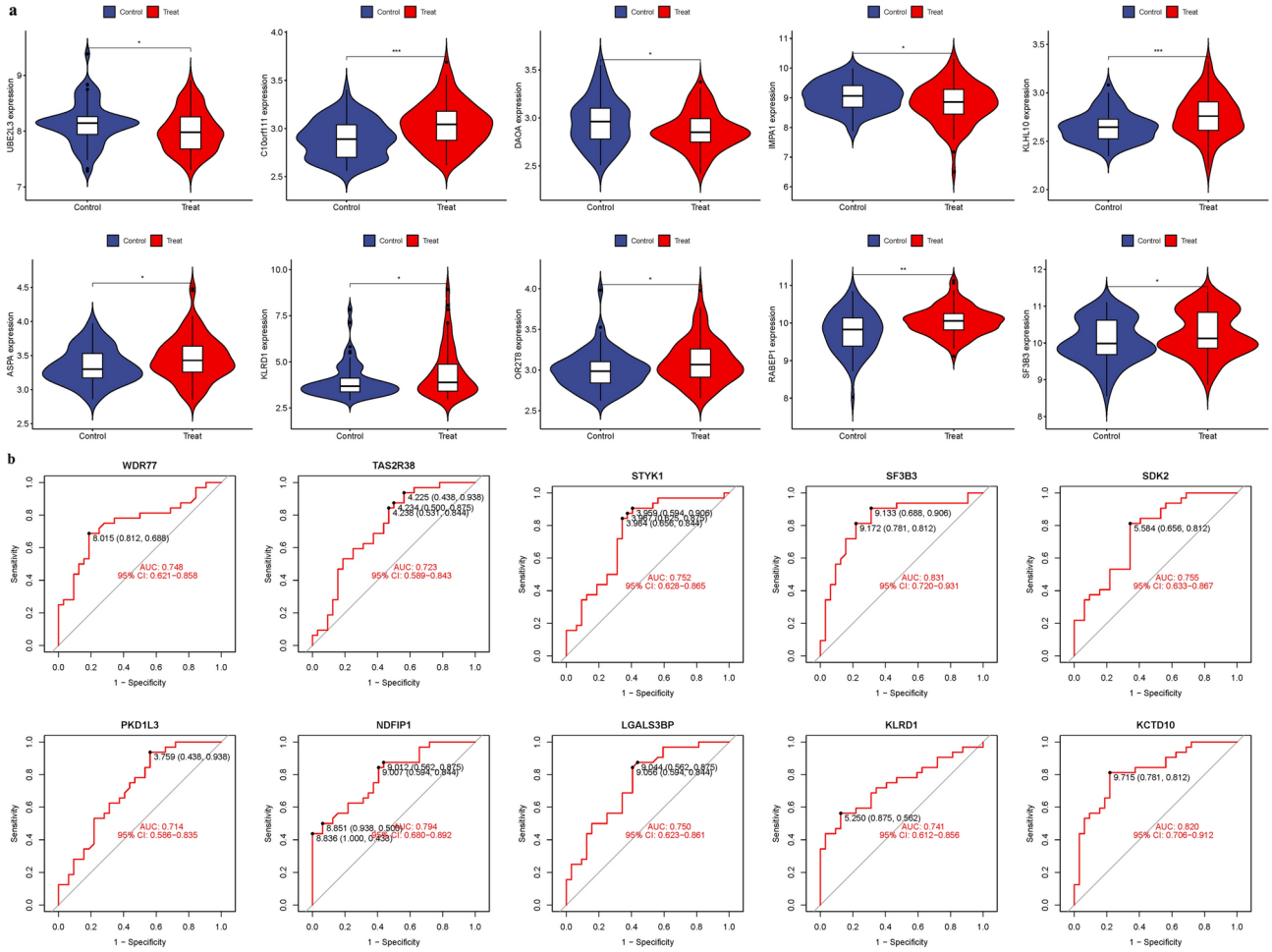

Fig. 6. Validation of Hub Genes. (**a**) Expression of 23 hub genes in GSE9820 analysis. (**b**) ROC of 23 hub genes.

contributing to vascular remodeling and plaque stability. Meanwhile, low expression, associated with immune activation and granule function, aligns with heightened inflammatory responses and leukocyte infiltration—hallmarks of AS progression. KEGG pathway analysis revealed that high *KCTD10* expression groups showed significant enrichment in pathways like dilated cardiomyopathy, hypertrophic cardiomyopathy hcm, olfactory transduction. Low expression groups exhibited enrichment in pathways associated with chemokine signaling pathway, hematopoietic cell lineage, lysosome (Fig. 8b, Table S4). For the GSVA, we utilized tools such as reshape2 for data restructuring, ggpubr for publication-quality visualizations, along with limma, GSEABase, and GSVA packages for robust analytical assessments. This analysis aimed to pinpoint functional alterations in the *KCTD10* DEGs. In GO terms, the high expression group showed enrichment in processes such as BP atrial cardiac muscle cell to av node cell signaling, BP atrial cardiac muscle cell membrane repolarization, BP noradrenergic neuron differentiation, MF mhc class ii receptor activity, BP membrane repolarization during atrial cardiac muscle cell action potential, BP glyceraldehyde 3 phosphate metabolic process, CC aggresome (Fig. 8c). KEGG analysis highlighted enrichment in pathways including vascular smooth muscle contraction, nod like receptor signaling pathway, cytosolic dna sensing pathway, tgf beta signaling pathway, circadian rhythm mammal, complement and coagulation cascades (Fig. 8d).

Gene regulatory networks and drug enrichment analysis

To unravel the molecular mechanisms underpinning KCTD10 function, a comprehensive gene regulatory network was constructed, revealing key interactions between KCTD10 and genes such as NOTCH1, POLD2, CD2AP, B9D1, and KCTD13 (Table S5, Fig. 9). These genes are intricately linked to processes of tissue repair and inflammation, suggesting that KCTD10 acts as a central regulator in pathways critical to vascular homeostasis and immune modulation. The regulatory connections highlight KCTD10's potential role in orchestrating cellular responses that influence the pathogenesis of AS. Specifically, KCTD10 may modulate endothelial repair, inflammatory cascades, and vascular remodeling through these interactions. Expanding on these findings, the study identified a network of drugs associated with KCTD10, including yohimbic acid, pimozide, copper sulfate, and betulin (Fig. 10c). Among these, yohimbic acid emerged as the most enriched candidate (Fig. 10a-b), leading to molecular docking studies that revealed a potential binding interaction with KCTD10 (Fig. 10d, Table 3).

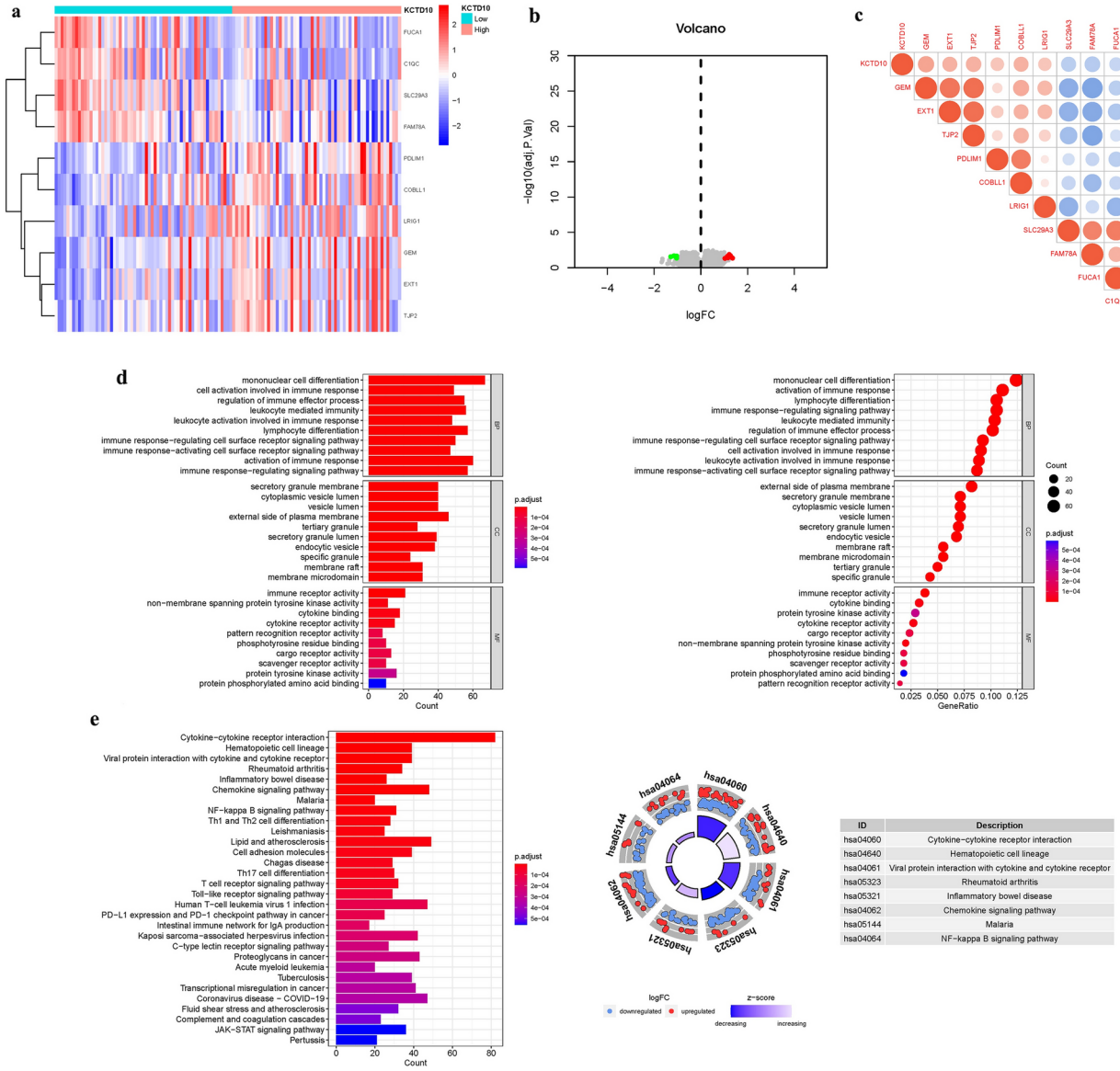

Fig. 7. DEG Identification and Enrichment analysis of *KCTD10*. (**a**): Heatmap. (**b**): Volcano map. (**c**): Correlation matrix diagram. (**a**): The GO circle illustrates the barplot, chord, circos, and cluster of the selected gene's logFC. (**b**): The KEGG barplot, chord, circos, and cluster illustrates the scatter map of the logFC of the indicated gene.

These results provide a foundation for exploring the pharmacological modulation of KCTD10 as a therapeutic strategy. We hypothesize that KCTD10 contributes to AS progression by regulating genes and pathways involved in tissue repair and inflammation, processes that underpin endothelial dysfunction, immune cell infiltration, and plaque development. The potential interaction with yohimbic acid further suggests that KCTD10-targeting drugs could mitigate these pathogenic mechanisms. Future investigations should focus on validating these interactions and elucidating the therapeutic efficacy of KCTD10 modulation in AS, offering a promising avenue for intervention in this complex disease.

Immune landscape characterization

Figures 11 explore the immune landscape of AS, with a particular focus on *KCTD10* as a pivotal gene for investigating its role within the immune contexture of the disease. This analysis provides vital insights into patterns of immune infiltration, underscoring the immunological factors critical to the initiation and progression of AS. The analysis revealed significant disparities in immune cell infiltration linked to risk profiles associated with *KCTD10* expression. In the *KCTD10*-defined cohorts, marked differences were observed in the infiltration levels of T helper cells between the low and high-risk groups. These variances highlight a complex immune modulation in different risk strata. Conversely, aDCs, APC co inhibition, APC co stimulation, B cells, CCR, CD8 + T cells, Check – point did not exhibit significant differences in infiltration between the risk groups,

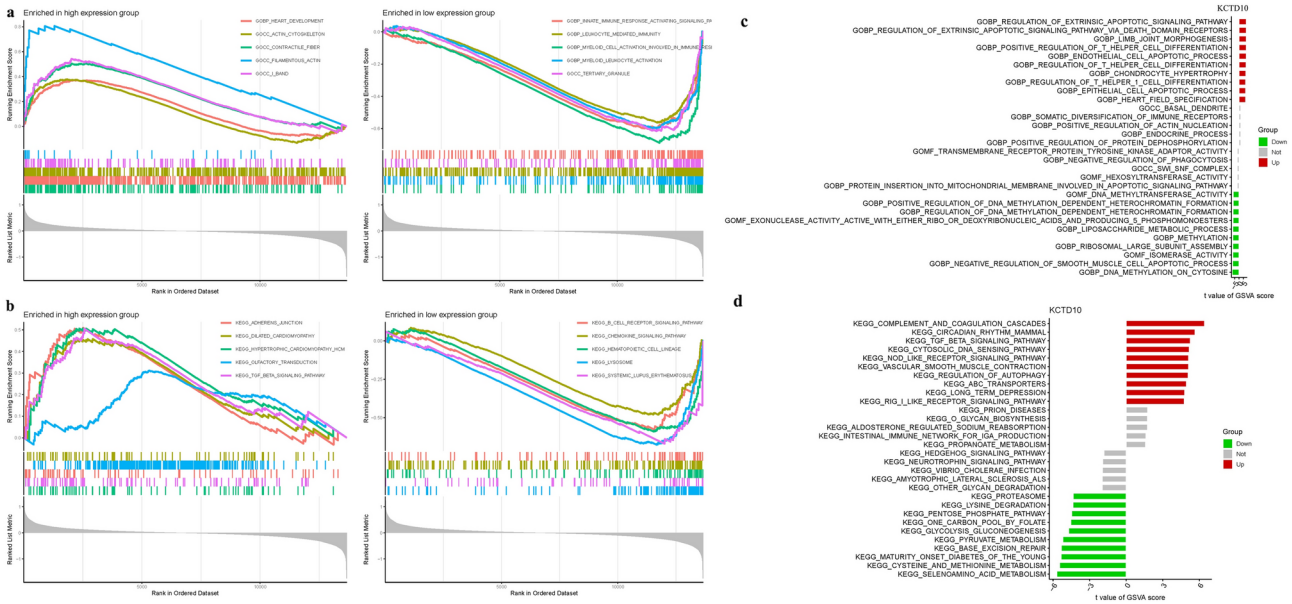

Fig. 8. GSEA and GSVA of Analysis in *KCTD10*. (**a**): GO. (**b**): KEGG. (**c**): GO. (**d**): KEGG.

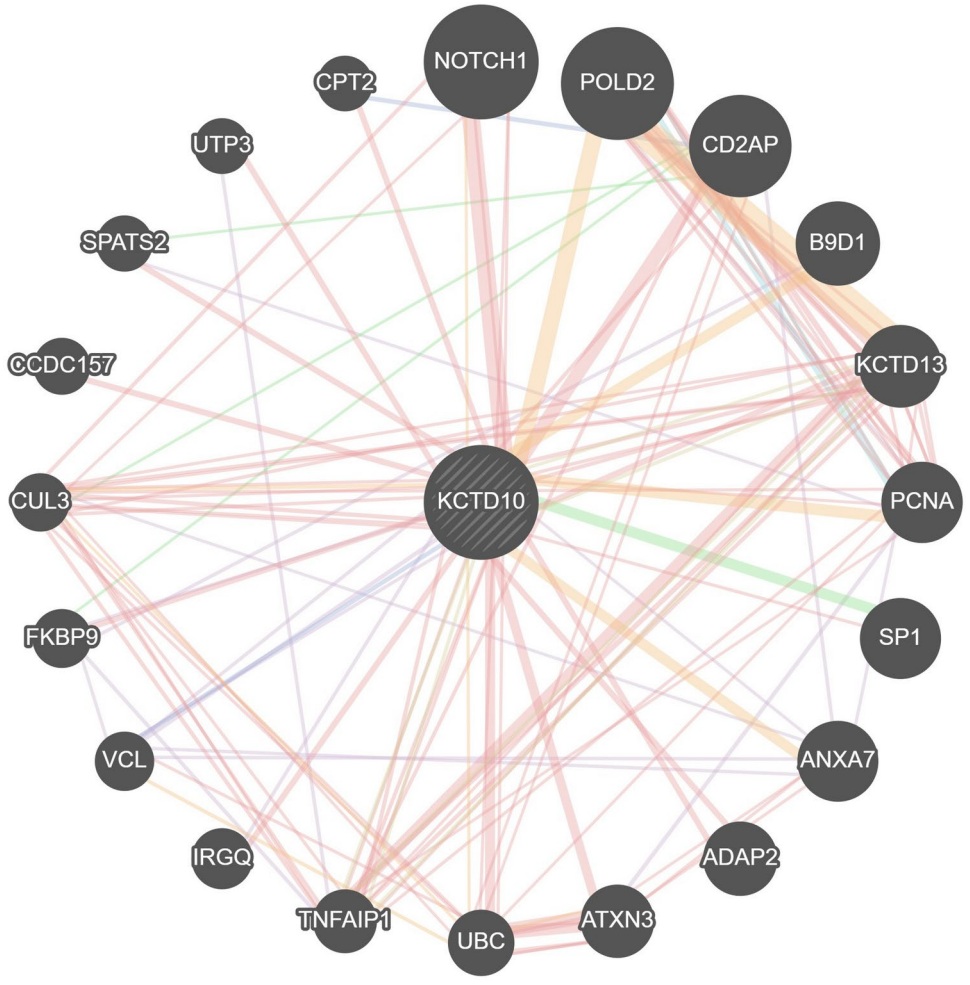

Fig. 9. Gene regulatory networks of KCTD10.

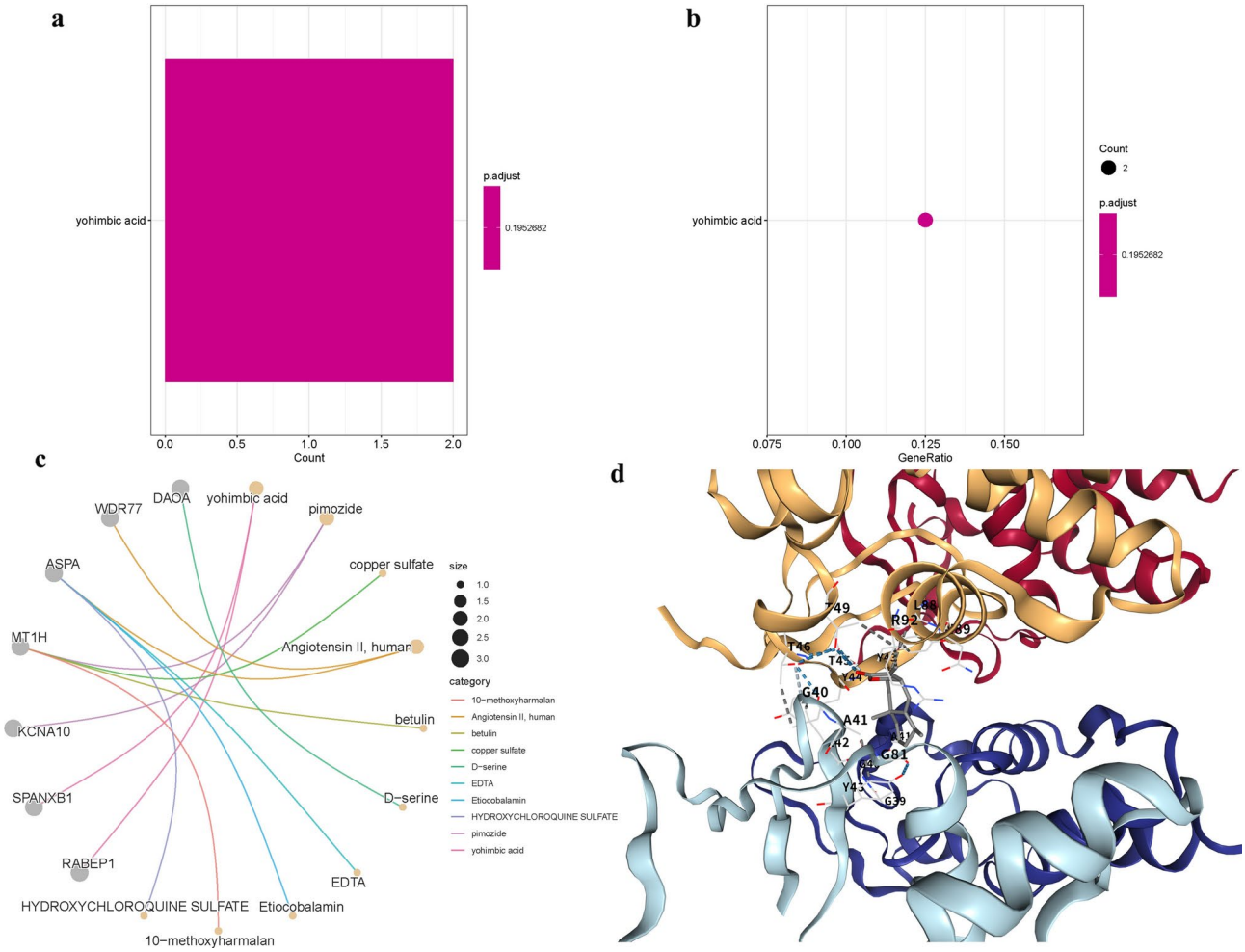

Fig. 10. Drug enrichment analysis and molecular docking. (**a**-**b**) GO. (**c**) network pf drugs. (**d**) Molecular docking.

CurPocket	Vina	Cavity	Center	Docking size	Contact
ID	score	volume (Å3)	(x, y, z)	(x, y, z)	residues
C1	−7.5	4334	16, 62, 16	28, 32, 35	View
C3	−6	434	−2, 72, 6	18, 18, 18	View
C4	−6	219	21, 82, 9	18, 18, 18	View
C2	−5.9	711	2, 76, 21	18, 18, 18	View
C5	−5.2	214	32, 69, 22	18, 18, 18	View

Table 3. Molecular docking of KCTD10 with yohimbic acid.

indicating a consistent involvement across the spectrum ($P > 0.05$) as detailed in Fig. 11a. This dichotomy in immune cell behavior underscores the nuanced role of *KCTD10* in modulating the immune environment in AS. B cells naive, Plasma cells, T cells CD4 memory resting, T cells CD4 memory activated, Macrophages M2, Dendritic cells activated, Neutrophils were highly expressed in the treat group. While, Dendritic cells resting, T cells follicular helper, T cells regulatory (Tregs), T cells gamma delta, NK cells resting, B cells memory did not exhibit significant differences in infiltration between the risk groups (Fig. 11b). In addition, we also constructed an immune infiltration correlation rectangle plot and heatmap (Fig. 11c-d). Through PCA analysis, immune-based patient categorization was again successfully executed (Fig. 11e). A Lollipop was created to display the expression patterns of Correlation Coefficient. Macrophages M1, T cells CD4 memory activated, Dendritic cells activated, Eosinophils, Plasma cells (Fig. 11f). Eosinophils and Plasma cells were shown to be positively associated with *KCTD10,* While, T cells CD4 naive was shown to be negatively associated with *KCTD10* (Fig. 11g). (Table.S5).

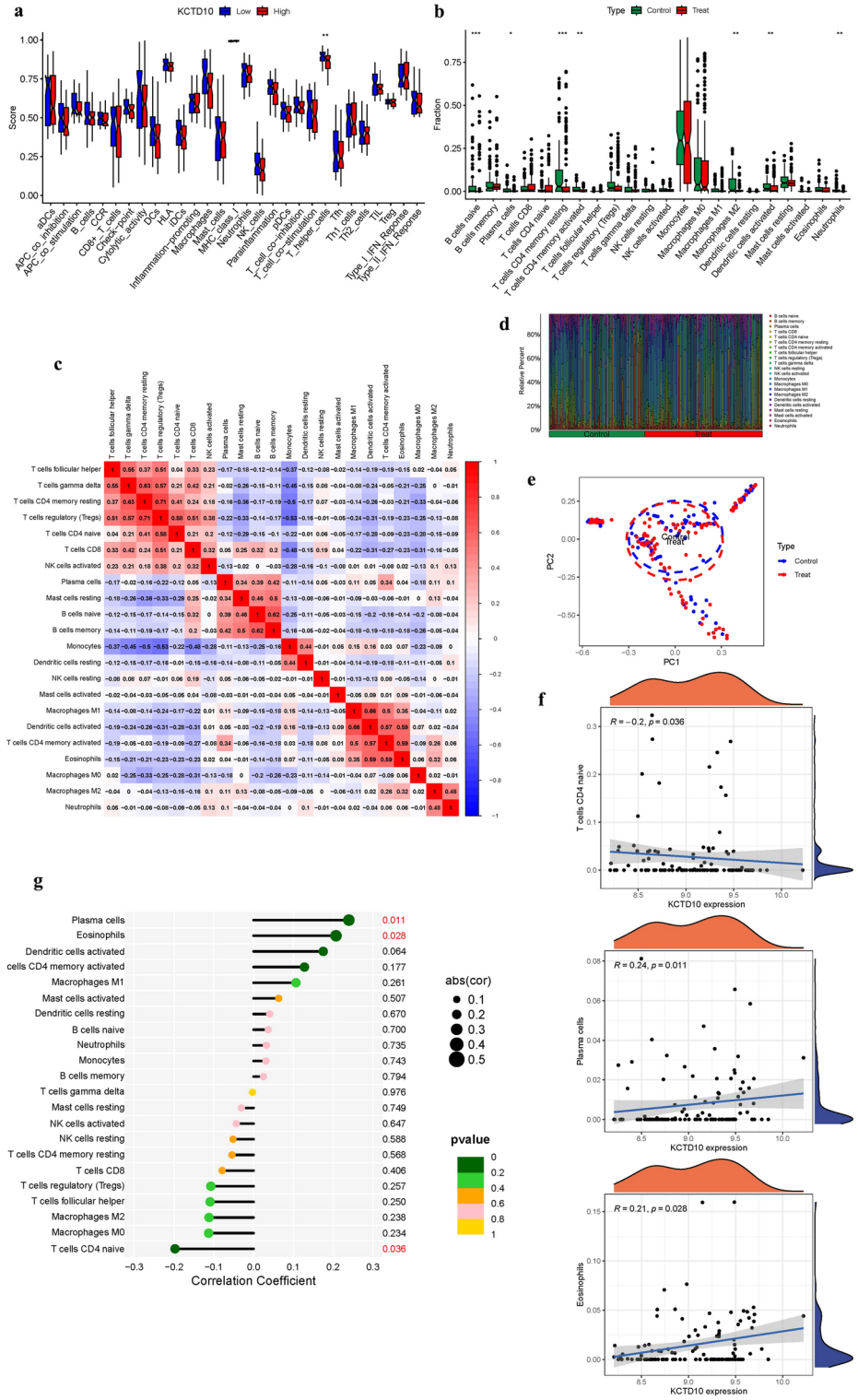

Fig. 11. Immune Landscape Characterization. (**a**) Expression of immune function. (**b**) Expression of immune cells (**c**) Correlation rectangle plot. (**d**) Heatmap. (**e**) PCA analysis. (**f**) The expression patterns of Correlation Coefficient. (**g**) Immune infiltration analyses.

Identification of common RNAs and construction of miRNAs-LncRNAs shared genes network

Fig. 12 uses *KCTD10* as a hub gene to investigate its expression dynamics within AS-associated miRNAs and lncRNAs, aiming to delineate its regulatory network. Three databases were searched for 49 miRNAs and 97 lncRNAs linked with AS (Table.S7a-b). The network of miRNAs-lncRNAs-genes was constructed by taking the intersection of them and shared genes (obtained by Lasso regression and SVM-RFE). Finally, the miRNAs-genes network included 79 lncRNAs (C10orf91, LINC01043, HP09025, LL22NC03-27C5.1, RP11-14P20.1, RP11-326C3.10, AP001476.4, RP4-737E23.2, RP11-102K13.5, MMP25-AS1, RP11-618K13.2, MUC2, CTD-3138B18.52, etc.), 19 miRNAs (hsa-miR-22-3p, hsa-miR-342-3p, hsa-miR-296-5p, hsa-miR-149-3p, hsa-miR-185-3p, hsa-miR-762, hsa-miR-302a-5p, hsa-miR-1-3p, etc.) (Fig. 12).(Table.S7). The identification of this extensive miRNA-lncRNA-gene network suggests a complex regulatory mechanism through which KCTD10 may influence key pathways involved in AS pathogenesis. Notably, KCTD10 appears to modulate inflammation, endothelial dysfunction, and vascular remodeling by interacting with specific miRNAs and lncRNAs. These interactions could impact the expression of genes involved in immune cell recruitment, lipid metabolism, and smooth muscle cell proliferation, all of which are central to the development and progression of AS. We hypothesize that KCTD10's role in AS is mediated by its regulation of these miRNAs and lncRNAs, which may in turn regulate the expression of critical genes involved in immune activation and vascular integrity. The therapeutic potential of targeting KCTD10, through modulation of its regulatory network, could offer a novel strategy to mitigate inflammation and plaque formation in AS. Further investigation is required to validate the functional significance of these miRNA-lncRNA-gene interactions and their therapeutic applicability in AS management.

Mendelian randomization analysis

In examining the direct linkage between the KCTD10 and AS incidence, a forest plot was utilized for visual illustration, revealing a general symmetry in the data. Through sensitivity analysis employing the "leave-one-out" technique, it was determined that the omission of any individual SNP had a minimal effect on the results of the inverse variance-weighted (IVW) analysis, indicating that the remaining SNPs closely mirrored the overall

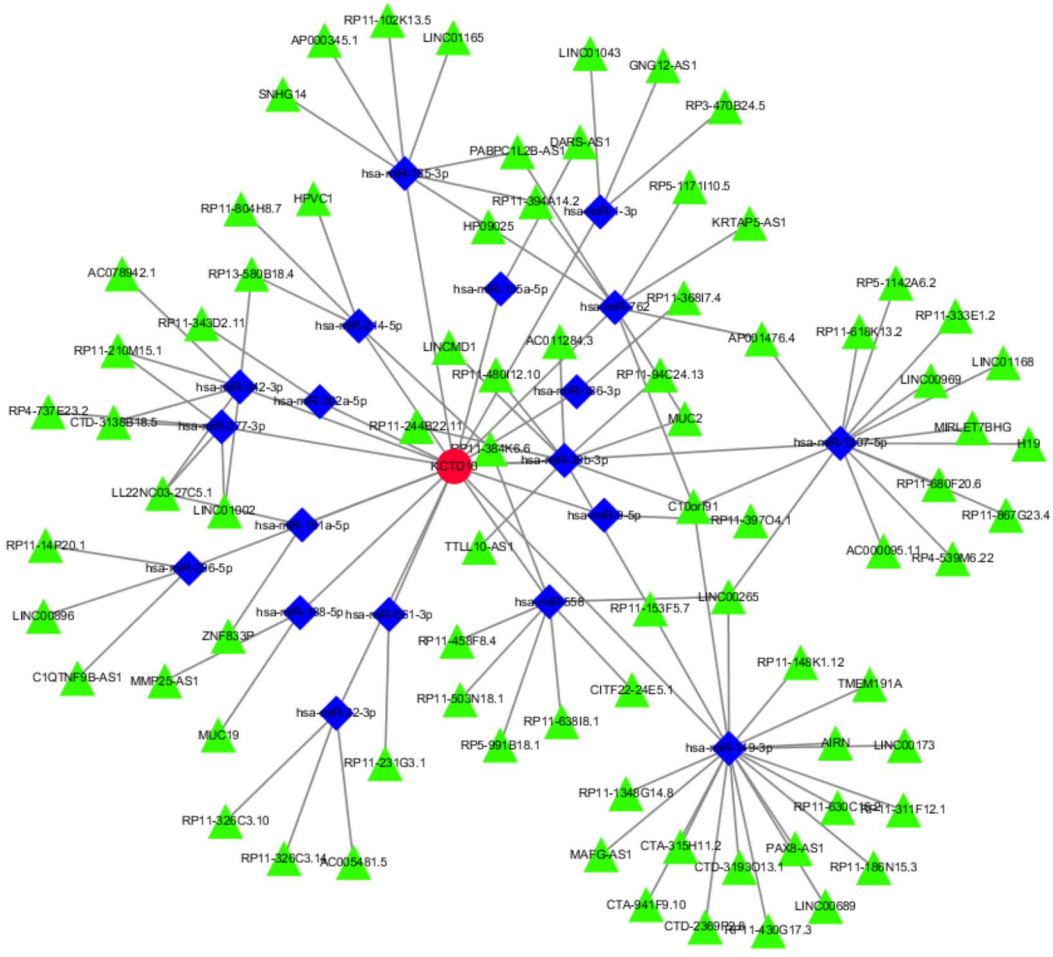

Fig. 12. miRNAs-LncRNAs shared Genes Network. Note: Red circles are mrnas, blue quadrangles are miRNAs, and green triangles are lncRNAs.

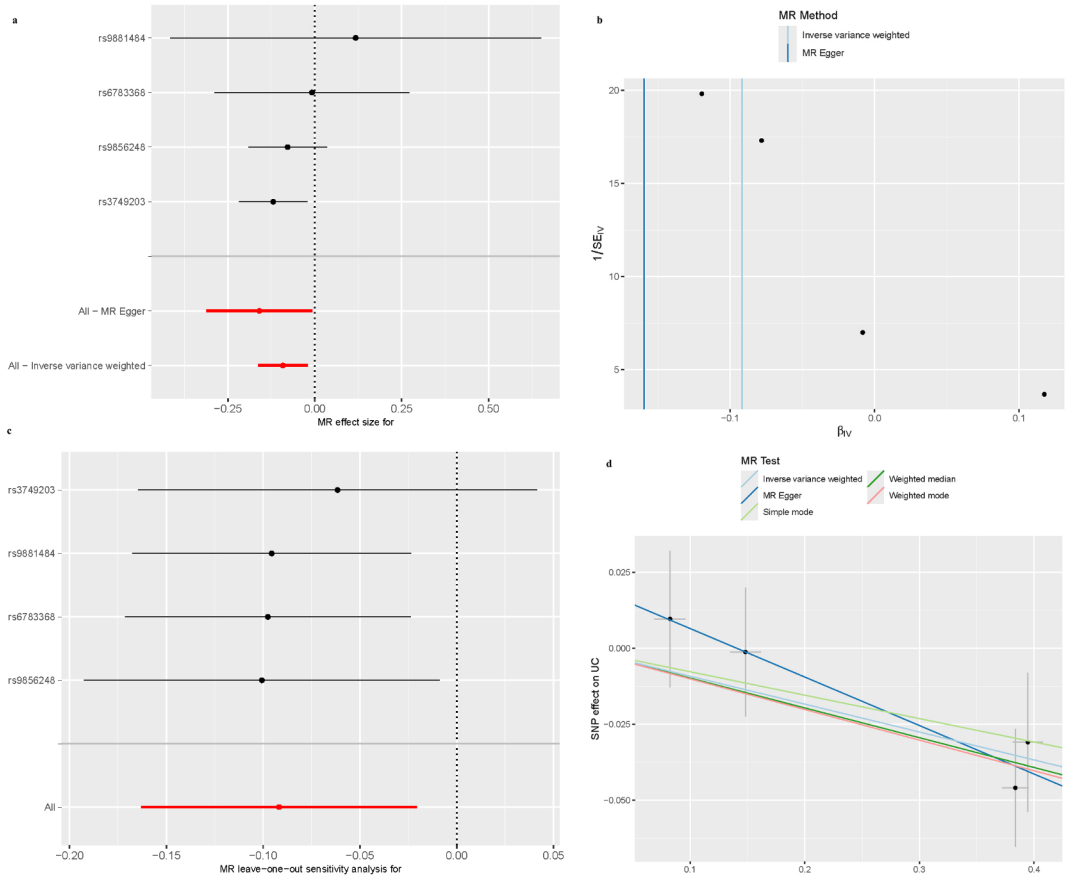

Fig. 13. Mendelian Randomization Analysis. (**a**) Correlation rectangle plot. (**b**) Heatmap. (**c**) The expression patterns of Correlation Coefficient. (**d**) SNP effect on AS.

dataset's findings. To further authenticate our outcomes, MR-Egger regression analysis was conducted, bolstering the integrity and reliability of our results and the chosen analytical framework (Fig. 13a–d).

Discussions

AS, a silent yet crucial contributor to vascular pathology, remains a primary etiological factor in cardiovascular disease-related morbidity and mortality. As such, the development of refined diagnostic tools to accurately assess atherosclerotic risk is of paramount importance. The progression of atherosclerotic plaques follows a complex trajectory, marked by immunological mechanisms akin to oncogenic processes. Therefore, a deep understanding of the immune- associated genes involved in plaque evolution is essential for advancing our knowledge of AS pathology. Within the cardiovascular milieu, KCTD10 emerges as a linchpin, underscored by its pivotal role in cardiac biology. This protein, a stalwart member of the KCTD gene family renowned for its T1 domains orchestrating potassium channel functionality, assumes a cardinal role in cardiac electrophysiology and myocardial dynamics. The symbiotic relationship between KCTD10 and the cardiac milieu is profound, chiefly through its regulatory sway over ion channels, pivotal for the maintenance of cardiac rhythmicity and contractility. Perturbations in potassium channel homeostasis, mediated by the regulatory machinations of KCTD10, precipitate arrhythmogenic propensities, thus underscoring the indispensability of this protein in preserving cardiac electrical stability. Moreover, the purview of KCTD10's influence extends to the molecular nuances underpinning cardiac metabolism and vascular integrity. Its intricate involvement in lipid and cholesterol metabolic cascades portends a broader purview within the spectrum of cardiovascular maladies, encompassing the genesis of atherosclerotic lesions culminating in coronary artery disease, a formidable harbinger of cardiac insufficiency. This study harnesses the synergistic potential of bioinformatics, combining model construction with computational analysis to provide a robust foundation for future basic and clinical research. The approach seeks to elucidate the complexities of AS and translate these findings into effective therapeutic strategies and clinically applicable frameworks.

In our comprehensive investigation of AS, we identified 10 DEGs associated with KCTD10. Through the integration of Lasso regression and SVM-RFE, we further refined this list to isolate a critical subset of genes implicated in AS pathogenesis. Cross-analysis revealed 11 central hub genes, including CYBB, SRSF5, CDC7, ARPC5L, and notably KCTD10 itself. Validation using external datasets confirmed the diagnostic relevance of these genes, highlighting their integral role within the complex molecular network underpinning AS. KCTD10 is particularly notable for its established function in modulating inflammation and immune responses. The

identification of these hub genes provides a solid foundation for future studies and emphasizes the need for deeper exploration into their regulatory mechanisms. KCTD10 has emerged as a pivotal determinant in the etiology of coronary AS, thereby underscoring its profound involvement in cardiovascular pathogenesis. As a constituent of the KCTD gene family, known for its intricate interplay with potassium channels to modulate their functionality, KCTD10 transcends conventional ion channel regulation, exerting its influence over expansive metabolic cascades, notably those governing lipid metabolism and cholesterol equilibrium[29]. Insightful investigations have elucidated the intricate molecular mechanisms whereby KCTD10 orchestrates lipid and cholesterol pathways, pivotal constituents in the genesis of atherosclerotic lesions[30]. Perturbations within these pathways culminate in the accretion of lipid-engorged macrophages and smooth muscle cells within arterial intima, hallmark manifestations of AS. By meticulously regulating these cardinal metabolic pathways, KCTD10 assumes a central role in the genesis and perpetuation of atherosclerotic plaques[31]. Moreover, the impact of KCTD10 on coronary AS extends beyond mere biological curiosity to encompass profound clinical ramifications. It presents an array of promising therapeutic targets for the management and prophylaxis of this malady, which stands as a foremost contributor to global morbidity and mortality, owing to its ultimate sequelae of myocardial infarction and stroke[32]. Ongoing investigations endeavor to unravel the nuanced interactions and ramifications of KCTD10 within cardiovascular milieu, affording deeper insights into its therapeutic potential in combating coronary AS. This ongoing scholarly pursuit underscores the pivotal role of KCTD10 in cardiovascular pathophysiology, particularly within the intricate tapestry of lipid regulation and atherogenesis[33]. Recent integrative analyses have positioned KCTD10 as a central hub within a comprehensive gene regulatory network linked to immune modulation, endothelial dysfunction, and vascular remodeling—key drivers of AS. Its role in regulating inflammatory responses, particularly through cytokine signaling and immune cell activation, marks it as a crucial mediator of the chronic inflammation that underpins AS progression. Additionally, KCTD10 influences essential signaling pathways related to smooth muscle cell proliferation, lipid metabolism, and extracellular matrix remodeling, all integral to plaque formation and vascular integrity. By interacting with specific miRNAs and lncRNAs, KCTD10 regulates genes involved in these processes, contributing to endothelial dysfunction, immune infiltration, and plaque destabilization characteristic of AS. Given its central role in these pathogenic mechanisms, KCTD10 presents as a promising therapeutic target for AS. Modulating KCTD10 expression or its downstream pathways could offer novel strategies to reduce inflammation, enhance vascular remodeling, and curb AS progression. Future research should focus on clarifying the molecular mechanisms through which KCTD10 influences AS pathology, as well as its potential as both a biomarker and therapeutic target in clinical applications. Our research highlights the critical function of KCTD10, alongside other differentially expressed genes, within the pathophysiology of AS. Data from the GSE9820 study further underscore the prognostic value of KCTD10-associated traits. However, genomic alterations linked to KCTD10 remain largely unexplored, revealing a significant gap in our knowledge. Addressing this gap is essential for unraveling the complex genomic interactions involving KCTD10, which could pave the way for novel therapeutic strategies in AS.

AS epitomizes chronic inflammatory diseases, deeply entwined with immune mechanisms, where the gradual development of arterial intimal plaques signals the advent of cardiovascular diseases. This pathophysiological progression begins with early inflammation, advancing through the complex evolution and eventual rupture of atherosclerotic plaques[34]. A myriad of immune cells, including monocytes/macrophages, T lymphocytes, dendritic cells, and mast cells, play a critical role in the development of AS, interacting dynamically and complexly. In the arterial environment, monocytes differentiate into macrophages, instigating lipid uptake and foam cell formation, hallmarks of atherosclerotic lesions[35]. CD4 + T cells amplify the inflammatory milieu, contributing to the proliferation of pro-inflammatory cytokines. Dendritic cells, positioned at the juncture of innate and adaptive immunity, regulate the immune response within the atherosclerotic lesion[36]. Mast cells exacerbate this process by discharging inflammatory mediators, intensifying inflammation and promoting plaque instability. The interplay between immune and vascular cells in AS is orchestrated by a complex network of cytokines, chemokines, and inflammatory mediators. Crucial pro-inflammatory cytokines like IL-1β, IL-6, and TNF-α play essential roles in endothelial activation and plaque progression[36]. Concurrently, chemokines direct the migration of immune cells to sites of inflammation, augmenting the inflammatory response. Toll-like receptors (TLRs) and NOD-like receptors (NLRs), recognizing PAMPs and DAMPs, initiate the inflammatory cascade characteristic of AS[37]. Immunomodulatory strategies targeting specific immune cells or inflammatory pathways provide innovative approaches to prevent and stabilize atherosclerotic plaques, potentially reducing cardiovascular events. In the treatment group, elevated expression was observed in naive B cells, plasma cells, resting CD4 memory T cells, activated CD4 memory T cells, M2 macrophages, activated dendritic cells, and neutrophils. In contrast, no significant differences were observed in resting dendritic cells, follicular helper T cells, regulatory T cells (Tregs), gamma-delta T cells, resting NK cells, or memory B cells between the risk groups. A Lollipop plot illustrating the correlation coefficient of immune cell expression patterns revealed positive associations between eosinophils, plasma cells, and KCTD10, while naive CD4 T cells were negatively correlated with KCTD10. By exploring the immunological nuances of AS, our research lays the foundation for innovative treatments that could significantly improve clinical outcomes, offering new avenues for managing this challenging condition.

The intricate interplay between AS and metabolic dynamics represents a burgeoning frontier in contemporary scientific inquiry. Recent strides, facilitated by the application of bioinformatics methodologies, have begun to unravel this multifaceted relationship[38–40]. A notable contribution to the field is Zemin Tian's seminal investigation, which elucidates the role of immunogenic cell death in endothelial cells in driving the chronic inflammation central to AS. Complementing Tian's work, Shuangyang Mo's research highlights the molecular and immunological similarities between non-alcoholic fatty liver disease and AS, identifying PLCXD3, CCL19, and PKD2 as key biomarkers linking these conditions. Meanwhile, Chi Ma's pioneering model based on autophagy-related genes, which identifies 19 significant genes, marks a significant advance in AS diagnostics

and therapeutics. Despite these substantial contributions, the relationship between purine metabolism and AS remains largely unexplored, with a notable gap in predictive models in this area. Our current research aims to fill this critical gap, offering new insights into this largely uncharted domain. Recognizing the limitations of our study, particularly in providing a comprehensive understanding of the underlying mechanistic pathways, we combine in vivo and in vitro approaches to gather valuable empirical data. These efforts, though still in their early stages, promise to lay the foundation for more extensive and integrated investigations into the pivotal role of KCTD10 in AS. Such research is poised to play a crucial role in incorporating these new findings into future therapeutic strategies, potentially enhancing treatment precision and efficacy.

Conclusions

This study investigates the intricate mechanisms underlying disease pathogenesis, with a particular focus on the critical role of KCTD10 in tissue repair, inflammation, and its prognostic significance in AS. Through the application of advanced predictive modeling, we delineate the transcriptional landscape of KCTD10, revealing significant expression differences between AS-affected and healthy tissues. These findings lay a robust foundation for future research, with the potential to inform the development of targeted therapeutic strategies for AS.

Data availability

The datasets generated during and/or analyzed during the current study are available in the appendix. The datasets generated and/or analysed during the current study are available in the [GEO] repository. https://www.ncbi.nlm.nih.gov/geo/'. Thanks to the KEGG database for the great support[41]. The citation guidelines: www.kegg.jp/kegg/kegg1.html.

Received: 19 June 2024; Accepted: 20 February 2025
Published online: 10 March 2025

References

1. De Bosscher, R. et al. Lifelong endurance exercise and its relation with coronary atherosclerosis. *Eur. Heart J.* **44**(26), 2388–2399 (2023).
2. Gallino, A. et al. Non-coronary atherosclerosis. *Eur. Heart J.* **35**(17), 1112–1119 (2014).
3. Sato, Y. et al. Sex differences in coronary atherosclerosis. *Curr. Atheroscler. Rep.* **24**(1), 23–32 (2022).
4. Al, R. M., Ahmed, A. I. & Al-Mallah, M. H. Evaluating coronary atherosclerosis progression among South Asians. *Atherosclerosis* **353**, 30–32 (2022).
5. Zhou, F. et al. Coronary atherosclerosis and chemotherapy: From bench to bedside. *Front. Cardiovasc. Med.* **10**, 1118002 (2023).
6. Honigberg, M. C. & Jowell, A. R. Accelerated coronary atherosclerosis after preeclampsia: Seeing is believing. *J. Am. Coll. Cardiol.* **79**(23), 2322–2324 (2022).
7. Ohmura, H. Contribution of remnant cholesterol to coronary atherosclerosis. *J. Atheroscler. Thromb.* **29**(12), 1706–1708 (2022).
8. Aengevaeren, V. L. et al. Exercise and coronary atherosclerosis: Observations, explanations, relevance, and clinical management. *Circulation* **141**(16), 1338–1350 (2020).
9. Ye, M. S. et al. KCTD10 regulates brown adipose tissue thermogenesis and metabolic function via Notch signaling. *J. Endocrinol.* **252**(3), 155–166 (2022).
10. Nagai, T., Mukoyama, S., Kagiwada, H., Goshima, N. & Mizuno, K. Cullin-3-KCTD10-mediated CEP97 degradation promotes primary cilium formation. *J. Cell Sci.* **131**, 24 (2018).
11. Kovacevic, I. et al. The Cullin-3-Rbx1-KCTD10 complex controls endothelial barrier function via K63 ubiquitination of RhoB. *J. Cell Biol.* **217**(3), 1015–1032 (2018).
12. Ma, T. et al. KCTD10 functions as a tumor suppressor in hepatocellular carcinoma by triggering the notch signaling pathway. *Am. J. Transl. Res.* **15**(1), 125–137 (2023).
13. Murakami, A. et al. Cullin-3/KCTD10 E3 complex is essential for Rac1 activation through RhoB degradation in human epidermal growth factor receptor 2-positive breast cancer cells. *Cancer Sci.* **110**(2), 650–661 (2019).
14. Jo, D. H., Kim, J. H. & Kim, J. H. Tumor environment of retinoblastoma, intraocular cancer. [Journal Article]. *Adv.. Exp. Med. Biol.* **1296**, 349–358. https://doi.org/10.1007/978-3-030-59038-3_21 (2020).
15. Jo, D. H., Kim, J. H. & Kim, J. H. Tumor environment of retinoblastoma intraocular cancer. *Adv. Exp. Med. Biol.* **1296**, 349–358 (2020).
16. Xia, L. et al. The cancer metabolic reprogramming and immune response. *Mol. Cancer* **20**(1), 28 (2021).
17. Zhang, Y. & Zhang, Z. The history and advances in cancer immunotherapy: understanding the characteristics of tumor-infiltrating immune cells and their therapeutic implications. *Cell. Mol. Immunol.* **17**(8), 807–821 (2020).
18. Peng, C. D. et al. Establishing and validating a spotted tongue recognition and extraction model based on multiscale convolutional neural network. *Digit. Chin. Med.* **5**(1), 49–58 (2022).
19. Wu, Z., Gao, Y., Cao, L., Peng, Q. & Yao, X. Purine metabolism-related genes and immunization in thyroid eye disease were validated using bioinformatics and machine learning. *Sci. Rep.* **13**(1), 18391. https://doi.org/10.1038/s41598-023-45048-9 (2023).
20. Wu, Z. et al. Bioinformatic validation and machine learning-based exploration of purine metabolism-related gene signatures in the context of immunotherapeutic strategies for nonspecific orbital inflammation. *Front. Immunol.* **15**, 1318316 (2024).
21. Wu, Z. et al. A novel Alzheimer's disease prognostic signature: identification and analysis of glutamine metabolism genes in immunogenicity and immunotherapy efficacy. *Sci. Rep.* **13**(1), 6895 (2023).
22. Wang, L., Wang, Y. & Bi, J. In silico development and experimental validation of a novel 7-gene signature based on PI3K pathway-related genes in bladder cancer. *Funct. Integr. Genom.* **22**(5), 797–811 (2022).
23. Blanchet, L. et al. Constructing bi-plots for random forest: Tutorial. *Anal. Chim. Acta* **1131**, 146–155 (2020).
24. Sanz, H., Valim, C., Vegas, E., Oller, J. M. & Reverter, F. SVM-RFE: selection and visualization of the most relevant features through non-linear kernels. *BMC Bioinform.* **19**(1), 432 (2018).
25. De Carvalho TR, Giaretta AA, Teixeira BF, Martins LB: new bioacoustic and distributional data on bokermannohyla sapiranga brandao et al., 2012 (anura: hylidae): revisiting its diagnosis in comparison with b. pseudopseudis (miranda-ribeiro, 1937). *zootaxa* 3746 2 383–392.
26. Chen, Y. & Wang, X. miRDB: an online database for prediction of functional microRNA targets. *Nucl. Acids Res.* **48**(D1), D127–D131 (2020).
27. Mon-Lopez, D. & Tejero-Gonzalez, C. M. Validity and reliability of the TargetScan ISSF Pistol & Rifle application for measuring shooting performance. *Scand. J. Med. Sci. Sports* **29**(11), 1707–1712 (2019).

28. Furio-Tari, P., Tarazona, S., Gabaldon, T., Enright, A. J. & Conesa, A. spongeScan: A web for detecting microRNA binding elements in lncRNA sequences. *Nucl. Acids Res.* **44**(W1), W176–W180 (2016).
29. Pang, X. F., Lin, X., Du, J. J. & Zeng, D. Y. Downregulation of microRNA-592 protects mice from hypoplastic heart and congenital heart disease by inhibition of the notch signaling pathway through upregulating KCTD10. *J. Cell. Physiol.* **234**(5), 6033–6041 (2019).
30. Feng, Y., Wang, C. & Wang, G. Inhibition of KCTD10 affects diabetic retinopathy progression by reducing VEGF and affecting angiogenesis. *Genet. Res. (Camb)* **2022**, 4112307 (2022).
31. Maekawa, M. & Higashiyama, S. KCTD10 biology: An adaptor for the ubiquitin E3 complex meets multiple substrates: Emerging divergent roles of the cullin-3/KCTD10 E3 ubiquitin ligase complex in various cell lines. *Bioessays* **42**(8), e1900256 (2020).
32. Cheng, J. et al. KCTD10 regulates brain development by destabilizing brain disorder-associated protein KCTD13. *Proc. Natl. Acad. Sci. U S A* **121**(12), e1979260175 (2024).
33. Maekawa, M. et al. Cullin-3/KCTD10 complex is essential for K27-polyubiquitination of EIF3D in human hepatocellular carcinoma HepG2 cells. *Biochem. Biophys. Res. Commun.* **516**(4), 1116–1122 (2019).
34. Fan, L. et al. High-dimensional single-cell analysis delineates peripheral immune signature of coronary atherosclerosis in human blood. *Theranostics* **12**(15), 6809–6825 (2022).
35. Boccara, F. & Cohen, A. Immune activation and coronary atherosclerosis in HIV-infected women: where are we now, and where will we go next?. *J. Infect. Dis.* **208**(11), 1729–1731 (2013).
36. Song, K., Li, L., Sun, G. & Wei, Y. MicroRNA-381 regulates the occurrence and immune responses of coronary atherosclerosis via cyclooxygenase-2. *Exp. Ther. Med.* **15**(5), 4557–4563 (2018).
37. Pereyra, F. et al. Increased coronary atherosclerosis and immune activation in HIV-1 elite controllers. *Aids* **26**(18), 2409–2412 (2012).
38. Liao, Y. et al. Lipid metabolism patterns and relevant clinical and molecular features of coronary artery disease patients: an integrated bioinformatic analysis. *Lipids Health Dis.* **21**(1), 87 (2022).
39. Chen, H. et al. Negative correlation between endoglin levels and coronary atherosclerosis. *Lipids Health Dis.* **20**(1), 127 (2021).
40. Zhang, X., Sun, R. & Liu, L. Potentially critical roles of TNPO1, RAP1B, ZDHHC17, and PPM1B in the progression of coronary atherosclerosis through microarray data analysis. *J. Cell. Biochem.* **120**(3), 4301–4311 (2019).
41. Tanabe M, Kanehisa M Using the KEGG database resource *Curr Protoc Bioinformatics* 2012 Chapter 1:1–12.

Author contributions
Xiaomei Hu and Fanqi Liang drafted and revised the manuscript. Xiaomei Hu and Fanqi Liang were in charge of data collection. Xiaomei Hu and Man Zheng were in charge of design of frame. Shanxi Wang and Juying Xie conceived and designed this article, in charge of syntax modification and revised of the manuscript. All the authors have read and agreed to the final version manuscript.

Funding
Hunan Graduate Research Innovation Program (No.CX20230818); Xiangnan University First-class Undergraduate Program Reform Project (2021–11).

Declarations

Competing interests
The authors declare that they have no conflict of interest.

Ethics approval
This manuscript is not a clinical trial, hence the ethics approval and consent to participation are not applicable.

Consent for publication
All authors have read and approved this manuscript to be considered for publication.

Additional information
Supplementary Information The online version contains supplementary material available at https://doi.org/10.1038/s41598-025-91376-3.

Correspondence and requests for materials should be addressed to J.X. or S.W.